International Journal of Energy Production and Management
Vol. 9, No. 3, September, 2024, pp. 121-130
Journal homepage: http://iieta.org/journals/ijepm

Performance Analysis of One Stage Anaerobic Digester Before and After Restating to Production Biogas/Biomethane

Atheer S. Hassoon[1*], Fawziea M. Hussien[2], Johain J. Faraj[2]

[1] Power Mechanics Engineering Department, Al-Musaib Technical College, Al-Furat Al-Awsat Technical University (ATU), Kufa 54001, Iraq
[2] Engineering Technical College, Middle Technical University, Baghdad 10074, Iraq

Corresponding Author Email: atheer.hassoon@atu.edu.iq

https://doi.org/10.18280/ijepm.090301

Received: 7 May 2024
Revised: 26 July 2024
Accepted: 12 August 2024
Available online: 26 September 2024

Keywords:
biogas, biomethane, Aspen Plus, energy efficiency, restarting time

ABSTRACT

In this work, biogas and biomethane production in a one-stage anaerobic digester (AD) are investigated. Four batch digesters were rotated at different speeds: 180 rpm for the first anaerobic digester (d1), 120 rpm for the second (d2), 60 rpm for the third (d3), and no speed at fourth digester (d4). Anaerobic digestion (AD) process of these digesters was thermophilic at 55°C and 1 bar. The substrates were three liters of water, 1.5 kg of potatoes (PT), and 1.5 kg of moist cow dung (CD). Rotating speed, pressure, temperature, residence time (RT), and restarting time were investigated in theoretical and experimental energies of an anaerobic digester (AD). The simulation of one-stage anaerobic digestion (AD) is studied using Aspen Plus software. The simulations showed that increasing AD pressure by one to three bars in one stage increased biomethane production by 32%. Increasing the temperature from 35 to 70 degrees increased biomethane output by 38%. Increasing AD residence duration to 384 days increased biomethane concentration by 52.23%. The move increased AD's gross heating value by 1.73%. The experiment's findings were obtained by holding the system at 1 bar, 55°C, and varying the restarting time between 6 and 24 hours. The average biogas volume increase between the 1st-AD and the 4th-AD before rest, after restarting, and after/before restating AD operations is 118%, 124.5%, and 10.96%, respectively. The average biogas concentration increases between the 1st-AD and the 4th-AD before restating, after beginning, and after/before restating AD processes is 17.31%, 20.65%, and 6.4%, respectively. For the first and fourth digestors, the absolute average deviation (AAD) of biomethane content was 3.78% and 3.21%, respectively. Experimental and simulation data agreed. Finally, digestor performance was directly proportional to AD restarting time for one stage, with the optimal interval after 6 hours.

1. INTRODUCTION

Many fields of technology, science, and society now emphasize energy production and employ. Increased energy generation is crucial due to 10 billion people on Earth by 2050 [1]. The looming global energy challenge necessitates investigating various options to increase the demand for biofuel liquid fuels produced from renewable biological sources, such as plants and algae, while also addressing environmental problems and their mitigation [2].

To protect fuel supply, energy prices, and the environment, nations with large natural gas and oil reserves must switch to renewable energy. Countries that have huge reserves of natural gas and oil must switch to renewable bioenergy sources to protect their fuel supply, energy costs, and the environment. To meet these demands, renewable bioenergy sources such as solar systems, biomass, wind turbines, and other technologies are being developed or used today can replace fossil fuels [3, 4].

Organic biomass can decompose into simpler molecules through biological processes. Biomass ranks high among clean energy sources in global energy supply [5-7]. Besides heating and fueling transportation, it generates electricity. Bioenergy accounted for 12% of world energy consumption (45.2 exajoules) in 2018 [8]. Increasing energy demand, fossil fuel pricing, dwindling reserves, and the environmental impact of fossil fuel burning have contributed to biomass's global importance as an environmentally beneficial energy source. Any biomass in anaerobic conditions will produce biogas.

Biogas is mostly carbon dioxide and methane, with some hydrogen sulfide and siloxanes. Burning methane, hydrogen, and carbon monoxide with oxygen is conceivable. Biogas is a biofuel for heat-requiring applications like cooking since it releases energy. Natural gas could power an engine that generates heat and electricity. Additionally, oil and gasoline engines can convert biogas into electricity [9, 10].

Rajendran et al. [11] developed an Aspen Plus model to forecast biogas output from any feedstock for process parameters with NRTL property method. Balanced digestors with continuous agitation simulated hydrolysis and other

processes. For 7 actual scenarios, we tested the model with feedstock concentrations of ± 5%, ± 10%, and ± 20%. The actual and Aspen Plus simulation results differed by 0.3% to 12.4%. When testing organic loading rate (OLR), RT, feedstocks, etc. process conditions, the experiment results matched the Aspen Plus model (P = 0.701). Rajendran et al. [11] verified their simulation model using seven scientific scenarios, however only two involved food garbage co-digested with other feedstocks (less than 30% volume). Thus, a chance to test the idea with food scraps exists. Al-Rubaye et al. [12] utilized Aspen Plus software to simulate the AD, cattle, and effluent. The simulation was built on a CSTR with 33 processes. It took 13 reactions for the hydrolysis process, where substrates were broken down by water. The temperature was between 50°C and 65°C (thermophilic), while the substrate levels were 5, 10, 20, and 30% of CD, cattle, and effluent. Running a simulation with various injection rates, pressures, and anticipated hydrogen additions allows investigators to determine their effect on methane gas production. According to the results, methane concentrations dropped as substrate levels and feed rates increased.

Ravendran et al. [13] simulated an AD with CD using Aspen Plus software to find the optimal OLR and operational pressure for high-quality methane gas. The simulation used three well-balanced reactors. Hydrolysis was the first reactor, acidogenesis and acetogenesis the second, and methanogenesis the last. Simulated feeding rates ranged from 0.03 to 0.51 L/day. Also simulated were hydrogen injection and six operational pressures. With 5% feedstock and 0.36 L/day feed flow, the high methane content was 74.2% with 180 m3/day, but with H_2 injection, it reached 85.2%. Menacho et al. [14] used Aspen Plus software to simulation AD. The conditions are temperatures (55°C), 1 atm pressure, 2 litter per day OLR, 51 litter per day, 40% to 60% fat levels and number of stages was two. The simulation outcome show that the average methane production was 75.95%. The simulation outcome displays that methane concentrations of 74.82% and 77.10% were reached when OLR of 21 L/day and a fat content of 40% were put together. The simulation result has a chance for use as an outline for further research of the relationship between fat quantity and AD. By combining the finding from both software, it has been calculated the average relative error percentage (0.0648%), which it below the engineering standard limitation.

Saber et al. [15] examined the AD efficiency of local organic matter mixed with partially decomposed CD, without the use of chemical ingredients, in a 50 L digester operating at high temperatures. The measurement of the process's performance is based on biomethane potential, organics elimination, and retention time. The biomethane production rate was 0.44 cubic meters of CH_4 per kilogram of VS. The duration of retention, as well as the AD stages, were decreased. The daily peak CH_4 production rate of 0.084 m^3 CH_4/(kg VS. day) was reached in just four days, whereas it took ten days to generate up 80% of the total biomethane yield. Over a period of five days, the efficiency of the method in removing volatile solids was found to exceed 35%. AD is well-suited for industrial-scale biowaste because to its high biomethane output.

Kitessa et al. [16] examined increased biogas production during AD by joining microalgae with wastewater. Three different ratios of wastewater to microalgae (3:0, 3:1, and 3:2) were employed in the laboratory batch digester for combined AD. The experiment lasted for 21 days and was carried out under average conditions. A wastewater to microalgae mixture ratio of 3:2 (60% wastewater volume to 40% microalgae volume) produced the most biogas, with a CH_4 methane content of 57.4%. These results indicate that co-digestion of microalgae and wastewater leads to increased biogas production, with biogas production rising proportionally to increasing amount of microalgae in the mixture.

Mecha and Kiplagat [17] investigated the properties of kitchen garbage and municipal solid waste with respect to their potential for biogas production, focusing on chemical and physical parameters. During ten days, the waste yielded 800 mL of biogas and 96.36 percent of volatile solids. By comparison, after a 28-day period, cooked rice waste yielded 83.00% of volatile solids and 2821 mL of biogas. Whereas cooked rice waste had a carbon to nitrogen ratio (C/N ratio) of 30, cabbage waste had a ratio of 13.9. Litter of cooked rice and cabbage had pH values of 7.2 and 6.2, respectively. The use of cooked rice waste to produce biogas via mono-digestion has shown superior yield compared to alternative substrates. Increasing the generation of biogas might need co-digestion of more substrates.

Alepu et al. [18] examined RT-influenced biogas production from sewage concentration bleed and adsorption. The study used three 900 mL CSTR digesters for 10, 20, and 30 days. Biogas methane concentration ranged from 60% to 70%, yielding 18 mL/d in reactor 1, 169 in reactor 2, and 114 in reactor 3. Reactor 3 consistently produced 166 mL/gCOD methane. Reactor 1 produced the least methane at 10 mL/g chemical oxygen. At reactor 1, OLR and shorter RT reduced VS. degradation and biogas output. This study recommends a 30-day RT and 0.6 gCOD(L.d) OLR for optimal methane production in CSTR-AD of coagulated and adsorbate sewage sludge.

Wei et al. [19] analyzed how RT affects waste AD degradation and restart. Decomposed hydrophilic molecules and volatile fatty acids increased in the liquid after 10 days of digestion at the lowest RT. Short RT hurt the digester. Caused by inefficient breakdown of Extracellular Polymers Substance (EPS), usually proteins. The digester degrades due to inefficient sludge EPS hydrolysis, especially for proteins and other chemicals. As RT decreased from 20 to 10 days, Methanosaetaceae aceticlastic species dropped from 36.3% to 27.6%. Hydrogenotrophic methanogens like methano-microbiales and methano-bacteriales rose from 30.4% to 38.3%. AD feed sludge proteins and fluorophores remained stable at high RT. Fulvic acid-like component fluorescence decreased significantly during digestion.

Pramanik et al. [20] evaluated a modest reactor's food waste AD. It uses advanced 16S rRNA sequencing to study reactor microbial populations. RT produced the most biogas at 1.01 L/g VS. and the highest COD removal of 95.84% and VS. of 92.7% after 124 days. Lowering RT to 62 days increases reactor ammonia and Volatile Fatty Acid (VFA) concentrations, lowering pH, biogas output, VS. removal efficiency, and Chemical Oxygen Diamond (COD). At 62 days, hydrogenotrophic methanogens decreased, slowing VFA breakdown and accelerating amino acid degradation, favoring VFA buildup. Methanogens failed to break down enough acetate throughout the 41-day RT, reducing process performance.

Zhang et al. [21] examined how OLR and RT effect food waste and sewage effluent thermophilic Co-AD. At 15 RT and 5.8 g.VS. L^{-1}. d^{-1} (OLR), maximum methane CH_4 generation was 328 ± 4 mL $CH_4.g^{-1}$ COD-fed. Improved acidogenesis,

acetogenesis, and methanogenesis increased production. Methanogenic substrates for CH_4 production have risen 5.2-fold using enzymes like acetate kinase. Syntrophic decarboxylation, acetate oxidation, reductive acetyl-CoA, and β-oxidation pathways facilitated trophic linkages with methanogens by symbiotic species The hydro-genotrophic Methanoculleus thermophilus metabolism and mixotrophic Methanosarcina thermophila abundance enhanced greatly. Different species' mutualisms shape heat-loving microbes.Feeding/idle period and restarted Digester

Okonkwo et al. [22] investigated biogas generation rates from organic wastes and weeds to determine the optimum poultry droppings-to-domestic waste ratio. Built digester for anaerobic breakdown of residential waste and weeds. The output of gas started on the 7th day and reached regularly, then quickly until the 18th day, when it peaked before falling. The 22-day experiment generated 1771 cm^3 of gas. Gas production peaked at 809 cm^3 in the sample with 50% poultry droppings and 50% weeds. This sample has the best C/N ratio of all created samples. Gas production started on the 2nd day after restarting the digester, compared to the 7^{th} day without restarting, and peaked sooner.

Li et al. [23] studied and examined three different feeding times: feeding daily (R1), feeding every 2 days (R2), and feeding every 3 days (R3), with the same amount of food given each time. The results indicate that R3 and R2 generated methane levels that were 11.1% and 8.4% higher, respectively, than R1. R3 showed higher rates of lignocellulose conversion and system stability, followed by R2 and R1. Reducing the duration of feeding resulted in increased variations in biogas production, VFA concentrations, and pH levels between each feeding event. It was found that bacteria and Firmicutes were more common in cases where feeding happened less often during the hydrolysis and acidogenesis processes. The microbial species, a hydrogenotrophic methanogen, was the prevailing genus of archaea in all reactors. Optimizing the feeding period can enhance the efficiency of the AD of maize.

Mohan and Swathi [24] analyzed how copper affects reactor chain restarting and stability following a six-month food-free phase. After restarting with copper, the reactor batch had a constant COD elimination rate of 98 ± 1.96%, indicating successful organic material removal. After restart, biogas generation was 0.218 cubic meters per kilogram of digested COD and copper removal was 81.5%. Copper accumulation inhibited methanogens, reducing methane production. However, the reactor chain remained stable and effluent characteristics fulfilled discharge standards. The restart effectively transitioned biomass from resting to active, regardless of copper. Over 35 days, copper restarted the reactor chain, demonstrating its durability and longevity.

Recently, numerous studies have focused on biogas production through anaerobic digestion (bio-AD). Research indicates that modifying feedstock and pretreatment can enhance biogas output. However, there is a notable gap in experimental research regarding the interruption and resumption of feed into bio-AD systems. Further work is required to improve the modeling, simulation, and numerical analysis in this area. The primary objective is to conduct experimental and simulation studies on bio-AD to explore how pausing and resuming feed impacts biogas production.

2. SIMULATION

The Aspen Plus software (version 12.1) is perfect for simulating the production of biogas/biomethane through AD, with accurate mass and energy balance calculations. The output data from Anerobic Digestor Model No. 1 (ADM1) can be used as input data for Aspen Plus software. The AD unit in Aspen Plus software has the ability to share data with ADM1, which is built in MATLAB, using an Excel sheet. This Excel sheet efficiently imports outcomes from the ADM1 modeling and easily transmits them to the AD unit in Aspen Plus software. Also, this data is utilized to simulate the energy demands and energy production of the system.

A few feedstock components in the Aspen Plus databank lack protein, keratin, and inert chemicals. Thus, Table 1 requires pseudocomponent items. Table 2 shows all CD + PT feedstock components.

Table 1. Pseudocomponent characteristics [25]

Component Name	Average NBP	Gravity	Molecular Weight
	K	Density kg/cum	
INERT	1000	3000	100
KERATIN	353.15	1430	116.39
PROTEIN	353.15	1430	367.42

Table 2. Select component in Aspen Plus [25]

Component ID	Component Name	Alias
ACETI-01	ACETIC-ACID	$C_2H_4O_2$-1
ALANI-01	ALANINE	$C_3H_7NO_2$
ARGIN-01	ARGININE	$C_6H_{14}N_4O_2$-N_2
ASPAR-01	ASPARTIC-ACID	$C_4H_7NO_4$
ETHYL-01	ETHYL-CYANOACETATE	$C_5H_7NO_2$
CELLU-01	CELLULOSE	CELLULOSE
METHA-01	METHANE	CH_4
CYSTE-01	CYSTEINE-E-2	$C_3H_6NO_2S$-E
CO_2	CARBON-DIOXIDE	CO_2
ETHANOL	ETHANOL	C_2H_6O-2
DEXTROSE	DEXTROSE	$C_6H_{12}O_6$
GLUTMAIC	L-GLUTAMIC-ACID	$C_5H_9NO_4$
L-GLU-01	L-GLUTAMIC-ACID	$C_5H_9NO_4$
GLYCEROL	GLYCEROL	$C_3H_8O_3$
GLYCINE	GLYCINE	$C_2H_5NO_2$-D1
FURFURAL	FURFURAL	$C_5H_4O_2$
H_2	HYDROGEN	H_2
H_2S	HYDROGEN-SULFIDE	H_2S
ISOLEICI	ISOLEUCINE	$C_6H_{13}NO_2$-I
GLUTA-01	GLUTARIC-ACID	$C_5H_8O_4$
LEUCINE	LEUCINE	$C_6H_{13}NO_2$
LINOLEIC	LINOLEIC-ACID	$C_{18}H_{32}O_2$
NH_3	AMMONIA	H_3N
OLEIC-01	OLEIC-ACID	$C_{18}H_{34}O_2$
1-HEX-01	1-HEXADECANOL	$C_{16}H_{34}O$
L-PHE-01	L-PHENYLALANINE	$C_9H_{11}NO_2$
PROLI-01	PROLINE	$C_5H_9NO_2$-N_8
PROPI-01	PROPIONIC-ACID	$C_3H_6O_2$-1
SERINE	SERINE	$C_3H_7NO_3$
SN-1--01	SN-1-PALMITO-2-LINOLEIN	$C_{37}H_{68}O_5$-1
THREO-01	THREONINE	$C_4H_9NO_3$
TRIOL-01	TRIOLEIN	$C_{57}H_{104}O_6$
TRIPA-01	TRIPALMITIN	$C_{51}H_{98}O_6$
VALINE	VALINE	$C_5H_{11}NO_2$
H_2O	WATER	H_2O
XYLOSE	D-XYLOSE	$C_5H_{10}O_5$
ISOBU-01	ISOBUTYRIC-ACID	$C_4H_8O_2$-4

All of the blocks as shown in the Figure 1 in Aspen Plus need property methods in order to give modeling results. This study uses NRTL (Non-Random Two Liquid) as its property method.

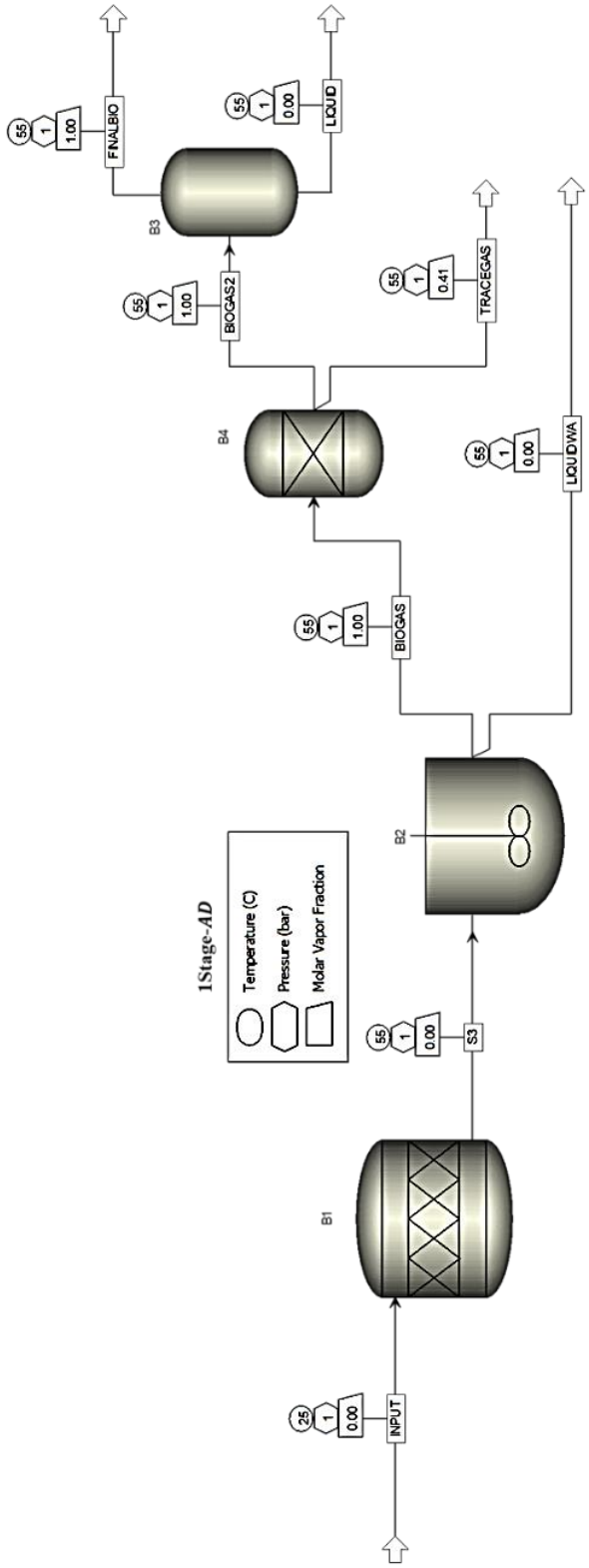

Figure 1. AD system with one stage

The National Renewable Energy Laboratory's (NREL) biofuels database includes active factors for different parts and combines the liquid and gas phases in the production of biogas and biomethane [26, 27].

Henry law has O_2, H_2S, CO_2, and CH_4 on its component list HC. If you want to figure out how well these parts dissolve in liquid, you can use Henry's rule. This study will also use the STEM-TABLE method to look at water properties.

The feedstock enters the block B1 that involve on the disintegration and hydrolysis AD process as illustrated in Figure 1. Where stoichiometric reactions with extent fraction conversion at (55℃, 1 bar) will be set inside it. Eleven hydrolysis chemical equations can be written as following:

$$\text{CELLU-01} + H_2O \rightarrow \text{DEXTROSE (MIX)} \quad (1)$$

$$\text{GLUTA-01} + H_2O \rightarrow 2.5\ \text{ACETI-01 (MIX)} \quad (2)$$

$$\text{GLUTA-01} + H_2O \rightarrow \text{XYLOSE (MIX)} \quad (3)$$

$$\text{XYLOSE} \rightarrow \text{FURFURAL (MIX)} + 3\ H_2O\ \text{(MIX)} \quad (4)$$

$$\text{CELLU-01} + H_2O \rightarrow 2\ \text{ETHANOL (MIX)} + 2\ CO_2\ \text{(MIX)} \quad (5)$$

$$2\ \text{ETHANOL} + CO_2 \rightarrow 2\ \text{ACETI-01 (MIX)} + CH_4\text{(MIX)} \quad (6)$$

$$\text{PROTEIN} + 6\ H_2O \rightarrow 6.5\ CO_2\ \text{(MIX)} + 6.5\ CH_4\text{(MIX)} + 3\ NH_3\ \text{(MIX)} + H_2S\ \text{(MIX)} \quad (7)$$

$$\text{KERATIN} + 0.334\ H_2O \rightarrow 0.045\ \text{ARGIN-01 (MIX)} + 0.048\ \text{ASPAR-01 (MIX)} + 0.047\ \text{THREO-01(MIX)} + 0.172\ \text{SERINE (MIX)} + 0.074\ \text{GLUTMAIC (MIX)} + 0.111\ \text{PROLI-01 (MIX)} + 0.25\ \text{GLYCINE (MIX)} + 0.047\ \text{ALANI-01 (MIX)} + 0.067\ \text{CYSTE-01 (MIX)} + 0.074\ \text{VALINE (MIX)} + 0.07\ \text{LEUCINE (MIX)} + 0.046\ \text{ISOLEICI (MIX)} + 0.036\text{L-PHE-01 (MIX)} \quad (8)$$

$$\text{TRIOL-01} + 3\ H_2O \rightarrow 3\ \text{OLEIC-01 (MIX)} + \text{GLYCEROL (MIX)} \quad (9)$$

$$\text{TRIPA-01} + 8.4375\ H_2O \rightarrow 4\ \text{GLYCEROL (MIX)} + 2.4375\ \text{1-HEX-01 (MIX)} \quad (10)$$

$$\text{SN-1--01} + 4.2875\ H_2O \rightarrow 2.2\ \text{GLYCEROL(MIX)} + 0.88785\ \text{1-HEX-01 (MIX)} + 0.9\ \text{LINOLEIC (MIX)} \quad (11)$$

Block B2 involves the acidogenesis, acetogenesis, and methanogenesis processes. Where chemical reactions with kinetics constant that it estimated according power law kinetic equation at (55℃, 1 bar) will be set inside it as seen in following equations. The acidogenesis process have four chemical equations can be reigning as the following:

$$\text{OLEIC-01} + 15.2359\ H_2O + 0.482\ CO_2 + 0.1701\ NH_3 \rightarrow 0.1701\ \text{ETHYL-01 (MIX)} + 9.02\ \text{ACETI-01 (MIX)} + 10.0723\ H_2\ \text{(MIX)} \quad (12)$$

$$\text{LINOLEIC} + 15.356\ H_2O + 0.482\ CO_2 + 0.1701\ NH_3 \rightarrow 0.1701\ \text{ETHYL-01 (MIX)} + 9.02\ \text{ACETI-01 (MIX)} + 10.0723\ H_2\ \text{(MIX)} \quad (13)$$

$$\text{1-HEX-01} + 14\ H_2O + 0.482\ CO_2 + 0.172667\ NH_3 \rightarrow 0.172667\ \text{ETHYL-01 (MIX)} + 7.80933\ \text{ACETI-01 (MIX)} + 15.036\ H_2\ \text{(MIX)} \quad (14)$$

$$\text{PROPI-01} + 0.06198\ NH_3 + 0.314336\ H_2O \rightarrow 0.06198\ \text{ETHYL-01(MIX)} + 0.9345\ \text{ACETI-01(MIX)} + 0.660412\ CH_4\ (\text{MIX}) + 0.160688\ CO_2\ (\text{MIX}) + 0.000552\ H_2\ (\text{MIX}) \quad (15)$$

The acetogenesis process have one equation can be written as:

$$\text{DEXTROSE} + 0.1115\ NH_3 \rightarrow 0.1115\ \text{ETHYL-01(MIX)} + 0.744\ \text{ACETI-01 (MIX)} + 0.5\ \text{PROPI-01 (MIX)} + 0.4409\ \text{ISOBU-01 (MIX)} + 0.6909\ CO_2\ (\text{MIX}) + 1.0254\ H_2O\ (\text{MIX}) \quad (16)$$

Finally, the methanogenesis process consist two chemical equations can be written as following:

$$\text{ACETI-01} + 0.022\ NH_3 \rightarrow 0.022\ \text{ETHYL-01 (MIXED)} + 0.945\ CH_4\ (\text{MIX}) + 0.066\ H_2O\ (\text{MIX}) + 0.945\ CO_2(\text{MIX}) \quad (17)$$

$$14.4976\ H_2 + 3.8334\ CO_2 + 0.0836\ NH_3 \rightarrow 0.0836\ \text{ETHYL-01 (MIX)} + 3.4154\ CH_4\ (\text{MIX}) + 7.4996\ H_2O\ (\text{MIX}) \quad (18)$$

The power law equation can be expression as the following formula:

$$k_f = k_{ff} \times \left(\frac{T}{T_o}\right)^n \times e^{-\left(\frac{E}{R}\right)\left[\frac{1}{\frac{T-1}{T_o}}\right]} \quad (19)$$

or

$$k_f = k_{ff} \times (T)^n \times e^{-\left(\frac{E}{TR}\right)} \quad (20)$$

where,

k_f is the kinetic factor (forward reaction) (s^{-1}),
k_{ff} is the frequency factor direction constant rate (s^{-1}),
T is the temperature of reaction (K),
T_o is the reference temperature (k),
n is the exponent of temperature (-), and
E is the active reaction energy (J/mole), and
R is the gas constant (8.314 J/mole).

The Eq. (19), use if known T_o, while Eq. (20) is use if T_o is unknow [28].

Eqs. (21) and (22) are used to calculated the reaction rate [29]:

$$R_i = \nu_i \times r \quad (21)$$

$$r_j = k_f \times \prod_i S_j^{-\nu_{ij}} \quad (22)$$

where, S_j is the species liquid concentration (mole/m^3), ν_{ij} is the stoichiometric reaction coefficient. Integrates block B1 with block B2 to form a single-stage AD.

3. METHODOLOGY AND EXPERIMENTAL INVESTIGATION

3.1 Experimental setup

Figure 2 illustrates the experimental setup used in this study, while Figure 3 provides a snapshot of the actual system.

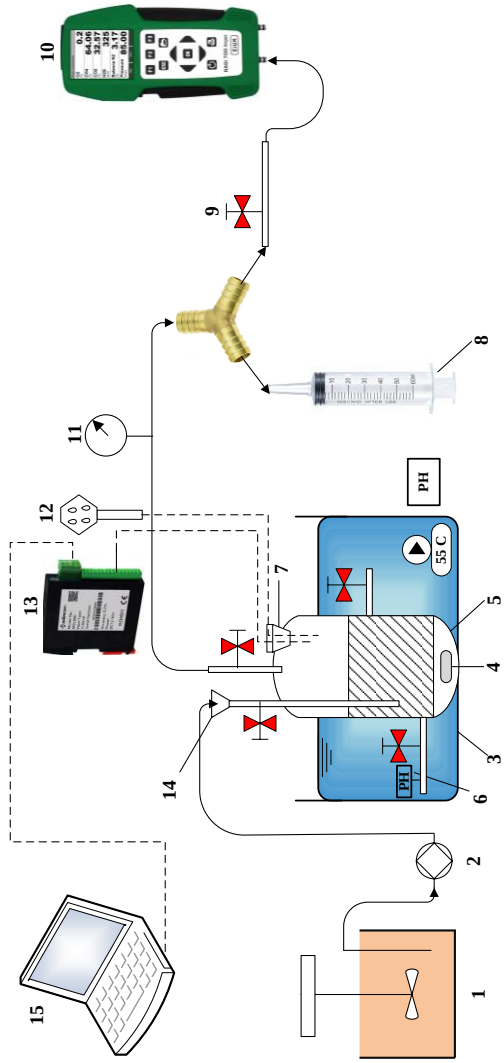

Figure 2. Experiment set-up schematic

Note: 1. Tank with handle mixer, 2. Pump, 3. Water bath, 4. Magnetic stirrer with capsules, 5. Bach-Co-AD, 6. pH-meter. 7. AD-Teflon cup, 8. Volume gas measurement, 9. Valves, 10. Gas analyzer, 11. Borden pressure gauge, 12. Digital humidity reader, 13. PLC-temperature reader, 14. Glass funnel, 15. Computer.

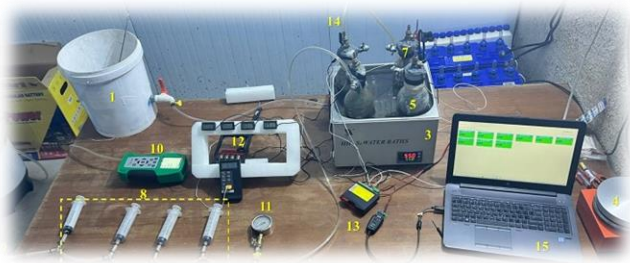

Figure 3. Photographical view of present system

Note: 1. Tank with handle mixer, 2. Pump, 3. Water bath, 4. Magnetic stirrer with capsules, 5. Bach-Co-AD, 6. pH-meter. 7. AD-Teflon cup, 8. Volume gas measurement, 9. Valves, 10. Gas analyzer, 11. Borden pressure gauge, 12. Digital humidity reader, 13. PLC- temperature reader, 14. Glass funnel, 15. Computer.

Four batch digesters are part of the system; Pyrex glass is heat- and chemical-resistant. They hold a 1000 millilitre capacity and 600 millilitres of substrate are used in them. The concentration of the gases % CH_4, % CO_2, % H_2S, and % O_2 was measured using the portable biogas analyzer model

(RASI700 BIOGAS), manufactured in the UK. 60 milliliter medical syringes to measure biogas volume, PLC data logger for read temperature, pressure measurement by Bourdon pressure gauge type EN837-1, and pH meter.

3.2 Tests procedure

The experimental work was done in Iraq, Babylon city, for 2023 summer season. The AD performances for generating biogas were thoroughly examined for different key variables. Each key variable was studied while keeping the others constant. Several variables affect the performance of biogas-AD:

- The effect of substrate circulation on the AD performance was studied in the range of 0 to 180 rpm, in step of 60 rpm.
- The effect of RT on the AD performance was studied for 384 hour (16 day).
- The effect of restating time after 6, 12, 18 and 24 hours on the performance of AD to produce biogas.

For the above variable keys, experimental procedures can be summarized as follows:

- Set up the four batch-AD bottles and check all measuring devices such as biogas analyzer and temperature reader.
- Collecting and mechanically preparing feedstocks (PT + CD).
- Mixing 1.5 kg of CD, 1.5 kg of PT, and 3 L of river water and wait until the mixture becomes homogeneous, then filled all four AD bottles.
- Utilize a magnetic stirrer to circulate the mixed feedstock at 0 rpm (d4), 60 rpm (d3), 120 rpm (d2), and 180 rpm (d1) to ensure optimal dispersion of bacteria within the anaerobic digester (AD).
- Fill each batch-AD with 600 mL of feedstock and set the batch AD on 55°C.
- Take and record readings such as temperature, pH, and biogas volume and biogas concentrations for each batch-AD every 24 hours.

Restart AD after 16 days and repeat point 5, and record data for every 6 hours.

3.3 Measurement uncertainty

Several variables, such as temperature, flowmeter, enthalpy, and liquid fraction, are used in error analysis to estimate measurement uncertainties in experimental data. The errors for these variables (W_R) can be evaluated as follows [30]:

$$W_R = \sqrt[2]{(\frac{\delta R}{\delta X_1} w_1)^2 + (\frac{\delta R}{\delta X_2} w_2)^2 + \cdots + (\frac{\delta R}{\delta X_n} w_n)^2} \quad (23)$$

Table 3. Error analysis

Independent Variables	Variable Errors
PLC-temperature readers (°C)	∓ 0.2
Humidity reader (%)	∓ 0.5
Pressure gage (bar)	∓ 0.01
Methane content (0-100%) VOL	∓ 0.2
Carbon dioxide content (0-100%) VOL	∓ 0.3
Oxygen content (0-25%) VOL	∓ 0.2
Hydrogen sulphide content (0-5000) ppm	∓ 5
Dependent Variables	**Variable Errors**
Enthalpy (kJ/kg)	∓ 0.034
Entropy (kJ/kg)	∓ 0.033
Gross heat (kJ/kg)	∓ 0.038

R is an operator that depends on the independent variables X_1, X_2, ..., X_n, and w_1, w_2, ..., w_n are the independent error variables. Table 3 presents a detailed analysis of the flaws and findings of the investigation.

4. RESULTS AND DISCUSSIONS

4.1 Simulation results

4.1.1 Variation of pressure

Figure 4 shows the effects of increasing operating pressures on biogas and biomethane generation. In one stage, the working pressure increased from 1 bar to 3 bar, resulting in an increase in biomethane composition from 52% to 69%. The percentage enhancement in biomethane production is 32%. The higher level of biomethane is because of the higher solubility of carbon dioxide as compared to methane, where the carbon dioxide to methane ratios is 0.7. Moreover, when the working pressure exceeds 3 bar, the composition of methane and its production rate start to decline. This is due to the inability of methanogen to efficiently create methane and its instability under high-pressure conditions [31].

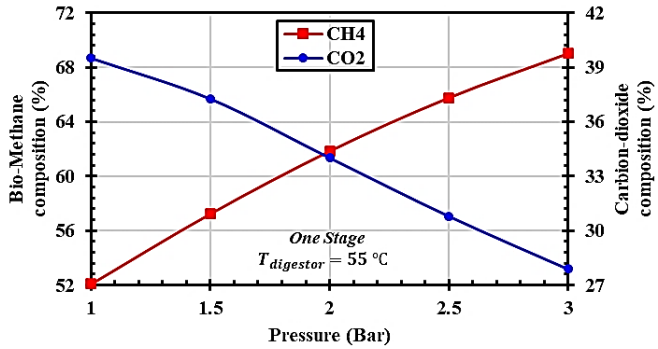

Figure 4. Pressure VS. biogas compositions

4.1.2 Variation of temperature

Figure 5 shows the temperature variation with RT in AD for biogas and biomethane production. The biomethane content increased from 42 to 58.1%, whereas at 1 bar, it was 52%. When the temperature rises from 35 to 70°C, biological and enzymatic processes within cells speed up, which is one of the reasons why the percentage of biomethane generation is growing [32]. The other reason is that the bacterial proliferation and metabolic activity of methanogen bacteria within AD are increasing, which is the first cause. The second factor, the solidity of carbon dioxide, also contributes to an increase in the generation of biomethane.

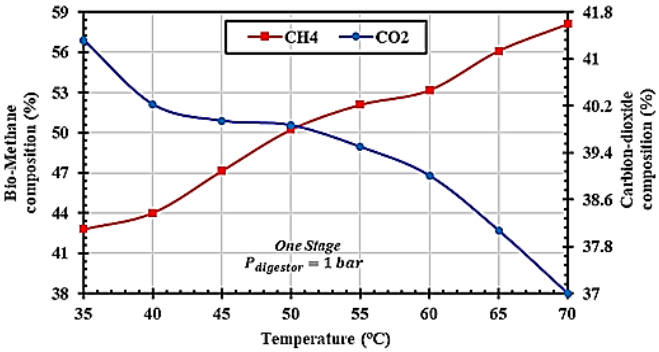

Figure 5. Temperature VS. biogas compositions

4.1.3 Variation of residence time (RT)

Increasing the RT to 16 days inside a 1-liter laboratory-AD under fixed conditions (1 bar and 55 degrees Celsius) resulted in an increase in biomethane concentration to 52.2%. Conversely, the carbon dioxide concentration decreased, as demonstrated in Figure 6. The decrease in carbon dioxide concentration (RT) led to an increase in the proliferation of methanogen bacteria, the organism responsible for methane generation. The consumption of carbohydrates, proteins, and other components occurred as a result of an increase in the rate of reaction (RT), which led to the total disintegration of the liquid phase.

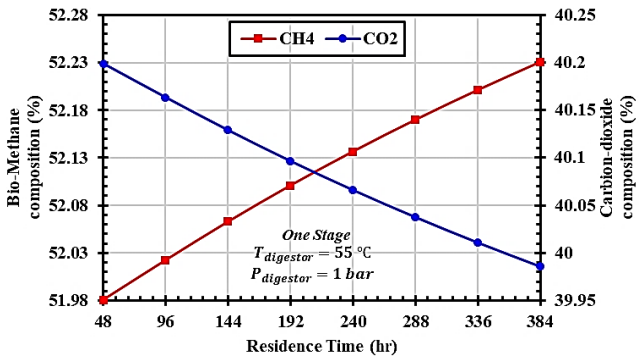

Figure 6. Pressure VS. biogas compositions

4.1.4 Variation of enthalpy and entropy

In thermodynamic terms, enthalpy is the total heat content of AD [10]. Figure 7 shows how, as residence time increases, so do the mass and mole enthalpy of biomethane. As high as (-7785 kJ/kg, -224869 kJ/kmole) is possible. In batch AD, endothermic mechanisms generate heat energy to support flame biomethane, or the enthalpy of methanogen reactions.

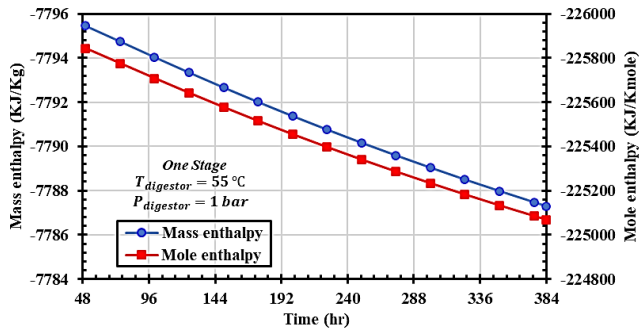

Figure 7. Residence time VS. mass and mole enthalpy

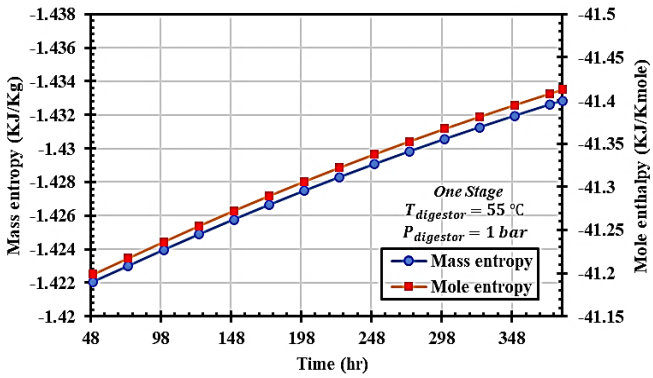

Figure 8. Residence time VS. mass and mole entropy

Entropy quantifies the level of unused energy inside a thermodynamic system. Figure 8 demonstrates the decline in both mass and mole entropy over time. The minimum values obtained are -1.435 kJ/kg and -41.46 kJ/kmole.

4.1.5 Variation of gross heating value

Figure 9 shows the variation in the gross heating value of biogas and biomethane over time. With RT, biomethane's gross heat increases, reaching 14978 kJ/kg for biogas and 15555 kJ/kg for biomethame gases. The rise in gross heat enhances the combustibility within the combustion chamber.

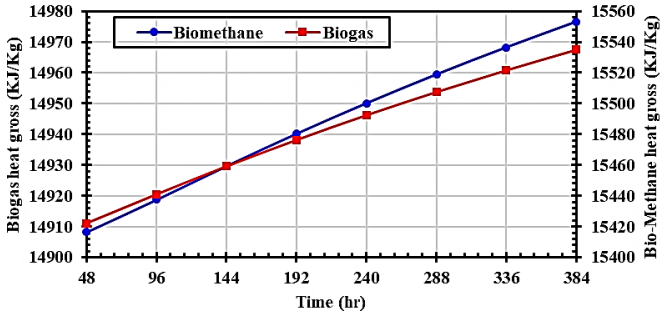

Figure 9. Residence time VS. biogas/biomethane gross heat

4.2 Experimental results

4.2.1 Variation of biogas production/before restarting AD

Before restating of one stage of AD, Biogas concentration begins after 48 hours, or two days. The biogas-producing bacteria was inactive between setup and production. Aerobic microorganisms in the digestor used all oxygen during this time. Biogas production began when oxygen ran out and acid-producing bacteria activated. Early biogas will be mostly carbon dioxide. The fermentation process will increase the quantity of subtracts necessary for the second step. Biomethane production begins then. Biogas biomethane content is expected to rise until it reaches its maximum generated biogas content. Biogas production increased gradually, then dramatically, reaching 51.16% CH_4 and 39.96% CO_2 at 8 days for 1st-AD at 180 rpm. For 2nd-AD with 120 rpm per day, the maximum biogas production is 50.09% CH_4 and 38.3% CO_2 at 8 days. While, the biogas output for 3rd-AD at 60 rpm per day climbed gradually at first, then rapidly until it reached its maximal value of 48.83% CH_4 and 39.02% CO_2 at 10 days. Finally for 4th-AD without rotational feedstock, the maximum biogas production occurs after 10 days, where it reaches up to 44.56% CH_4 and 35.2% CO_2, as shown in Figure 10. All anaerobic digesters (AD) utilize a magnetic stirrer with bars to spin the feedstocks, achieving homogeneity and ensuring optimal dispersion of bacteria.

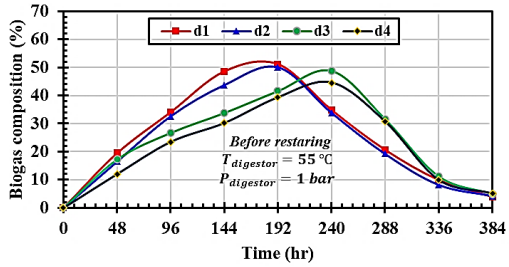

Figure 10. Residence time VS. biogas composition before restarting

4.2.2 Variation of biogas production/after restarting AD

After 384 hours, or sixteen days, methanogen-producing microorganisms in the Co-AD system do not activate bacteria. Reactivate methanogen-producing bacteria by injecting AD and feeding them at various times to start biogas production. After six, twelve, eighteen, and twenty-four hours, one-stage AD procedures restarted feedings. As the rotational speed decreased from 180 to zero, we slowed it by sixty revolutions per minute. Restarting feedstock injection in anaerobic digesters increased biogas production significantly.

Figure 11 shows that 56.5% of 1st-AD biogas contains methane (CH_4) and 45.21% carbon dioxide. Oxygen and hydrogen sulphide also contribute slightly.

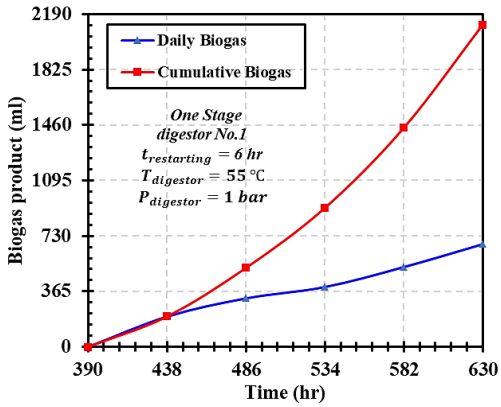

Figure 11. Residence time VS. biogas volume production for 1st-AD after 6 hours

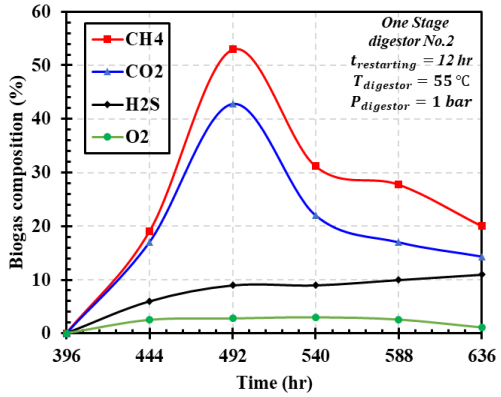

Figure 12. Residence time VS. biogas volume production for 2nd-AD after 12 hours

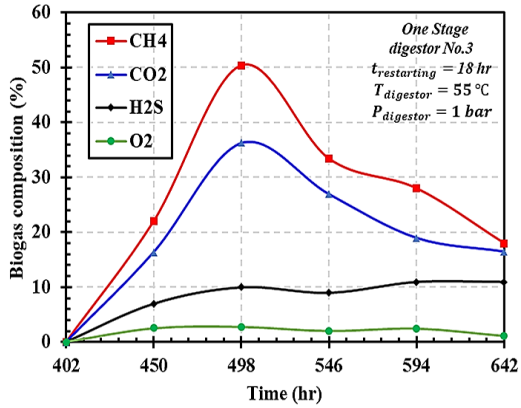

Figure 13. Residence time VS. biogas volume production for 3rd-AD after 18 hours

For 2nd-AD, with one stage at 120 rpm and restarting time after 12 hours, it can be noted that the maximum biogas production is 52.94% CH_4 and 42.8% CO_2, with a small amount of O_2 and H_2S, as shown in Figure 12.

The maximum production of biogas in the 3rd-AD stage AD with 60 rpm and 18 hours of restarting feeding time is 50.4% CH_4 and 36.32% CO_2, respectively. Where the maximum point of biogas production occurs after 6 days, as shown in Figure 13.

As shown in Figure 14, the biogas output reached its highest point after 24 hours of restarting the 4th-AD in one stage with no revolutions per minute (rpm). The output reached 44.5% methane (CH_4) and 34% carbon dioxide (CO_2) at its peak. It is possible to quantify minute quantities of other gases, such as oxygen (O_2) and hydrogen sulphide (H_2S), with the help of the biogas analyzer.

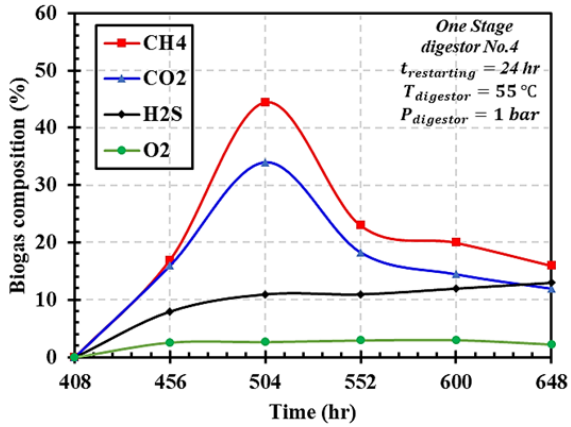

Figure 14. Residence time VS. biogas volume production for 4th-AD after 24 hours

4.3 Validation

Figure 15 illustrates a comparison of the biomethane content between experimental and simulation data. The experimental results are derived from data obtained through experimental measurements, whilst the simulation results are obtained by utilizing the mathematical model and solved using the Aspen Plus software.

The percentage of the absolute average deviation (AAD) [33] for determining the biomethane content in one-stage AD, the first AD has a rate of 3.78%, and the fourth AD has a rate of 4.35%.

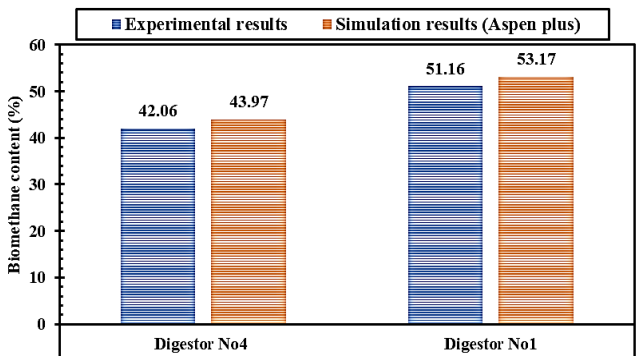

Figure 15. Comparison between simulation and experimental results for biomethane production

5. CONCLUSIONS

In summary, simulated and experimental examination of the influence of the idle period (restarting time RT) that occurs between the paused feeding and the resumed feeding of AD on the production of biogas/biomethane simultaneously with the subsequent restart is the primary focus of this work.

The simulation findings yield the following conclusions:

- The working pressure increased from 1 bar to 3 bar, increasing the biomethane composition from 52% to 69%, where the percentage enhancement in biomethane composition is 32%.
- The working temperature increased from 35 to 70℃, and the biomethane content climbed from 42 to 58.1%.
- Increasing the residence time up to 384 days led to an increase in the average biomethane concentration to 52.23%.
- Biomethane mass and mole enthalpy rise with increasing residence time, up to 384 days. The values may reach up to (-7785 kJ/kg, -224869 kJ/kmole), This means the biomethane reactions inside AD are exothermal for hydrolysis and acidogenesis process and endothermal for acetogenesis and methanogenesis process.
- Increasing the duration of residence time up to 384 days resulted in an increase in the average gross heat of biomethane.

The experimental findings under constant pressure (1 bar), thermophilic temperature (55℃), and variable rotational speed (180, 120, 60, and 0 rpm) showed the following:

- The average percentage enhancement in biogas volume before restarting Co-AD is 17.31%.
- The average percentage enhancement in biogas content after restarting Co-AD is 20.65%.
- The average percentage enhancement in biogas content before and after restarting Co-AD is 6.4%.

Finally, in further work, the finding results can be applied to other conditions, such as mesophilic temperature, and another stage, such as two stages instead of one stage of AD.

REFERENCES

[1] Osman, A.I., Chen, L., Yang, M., Msigwa, G., Farghali, M., Fawzy, S., Rooney, D.W., Yap, P.S. (2023). Cost, environmental impact, and resilience of renewable energy under a changing climate: A review. Environmental chemistry letters, 21(2): 741-764. https://doi.org/10.1007/s10311-022-01532-8

[2] Elsayed, M., Ran, Y., Ai, P., Azab, M., Mansour, A., Jin, K., Zhang, Y., Abomohra, A.E.F. (2020). Innovative integrated approach of biofuel production from agricultural wastes by anaerobic digestion and black soldier fly larvae. Journal of Cleaner Production, 263: 121495. https://doi.org/10.1016/j.jclepro.2020.121495

[3] Cardoso, J., Silva, V., Eusebio, D. (2019). Techno-economic analysis of a biomass gasification power plant dealing with forestry residues blends for electricity production in Portugal. Journal of Cleaner Production, 212: 741-753. https://doi.org/10.1016/j.jclepro.2018.12.054

[4] Tawfik, A., Eraky, M., Osman, A.I., Ai, P., Zhou, Z., Meng, F., Rooney, D.W. (2023). Bioenergy production from chicken manure: A review. Environmental Chemistry Letters, 21(5): 2707-2727. https://doi.org/10.1007/s10311-023-01618-x

[5] Salehi, R., Taghizadeh-Alisaraei, A., Shahidi, F., Jahanbakhshi, A. (2020). Potentiometric of bioethanol production from cantaloupe waste (Magassi Neishabouri Cultivar). Journal of the Saudi Society of Agricultural Sciences, 19(1): 51-55. https://doi.org/10.1016/j.jssas.2018.05.006

[6] Jahanbakhshi, A., Salehi, R. (2019). Processing watermelon waste using Saccharomyces cerevisiae yeast and the fermentation method for bioethanol production. Journal of Food Process Engineering, 42(7): e13283. https://doi.org/10.1111/jfpe.13283

[7] Heidari-Maleni, A., Mesri-Gundoshmian, T., Jahanbakhshi, A., Karimi, B., Ghobadian, B. (2021). Novel environmentally friendly fuel: The effect of adding graphene quantum dot (GQD) nanoparticles with ethanol-biodiesel blends on the performance and emission characteristics of a diesel engine. NanoImpact, 21: 100294. https://doi.org/10.1016/j.impact.2021.100294

[8] REN21. (2021). Renewables in cities-2021 global status report. https://www.ren21.net/cities-2021/pages/foreword/foreword/.

[9] Kabeyi, M.J.B., Olanrewaju, O.A. (2022). Biogas production and applications in the sustainable energy transition. Journal of Energy, 2022(1): 8750221. https://doi.org/10.1155/2022/8750221

[10] Obaideen, K., Abdelkareem, M.A., Wilberforce, T., Elsaid, K., Sayed, E.T., Maghrabie, H.M., Olabi, A.G. (2022). Biogas role in achievement of the sustainable development goals: Evaluation, challenges, and guidelines. Journal of the Taiwan Institute of Chemical Engineers, 131: 104207. https://doi.org/10.1016/j.jtice.2022.104207

[11] Rajendran, K., Kankanala, H.R., Lundin, M., Taherzadeh, M.J. (2014). A novel process simulation model (PSM) for anaerobic digestion using Aspen Plus. Bioresource Technology, 168: 7-13. https://doi.org/10.1016/j.biortech.2014.01.051

[12] Al-Rubaye, H., Karambelkar, S., Shivashankaraiah, M.M., Smith, J.D. (2019). Process simulation of two-stage anaerobic digestion for methane production. Biofuels, 10(2): 181-191. https://doi.org/10.1080/17597269.2017.1309854

[13] Ravendran, R.R., Abdulrazik, A., Zailan, R. (2019). Aspen Plus simulation of optimal biogas production in anaerobic digestion process. IOP Conference Series: Materials Science and Engineering, 702(1): 012001. https://doi.org/10.1088/1757-899x/702/1/012001

[14] Menacho, W.A., Mazid, A.M., Das, N. (2022). Modelling and analysis for biogas production process simulation of food waste using Aspen Plus. Fuel, 309: 122058. https://doi.org/10.1016/j.fuel.2021.122058

[15] Saber, M., Khitous, M., Kadir, L., et al. (2021). Enhancement of organic household waste anaerobic digestion performances in a thermophilic pilot digester. Biomass and Bioenergy, 144, 105933. https://doi.org/10.1016/j.biombioe.2020.105933

[16] Kitessa, W.M., Fufa, F., Abera, D. (2022). Biogas production and biofertilizer estimation from anaerobic co-digestion of blends of wastewater and microalgae. International Journal of Chemical Engineering, 2022(1): 3560068. https://doi.org/10.1155/2022/3560068

[17] Mecha, A.C., Kiplagat, J. (2023). Characterization of kitchen and municipal organic waste for biogas production: Effect of parameters. Heliyon, 9(5): e16360.

https://doi.org/10.1016/j.heliyon.2023.e16360
[18] Alepu, O.E., Li, Z., Ikhumhen, H.O., Kalakodio, L., Wang, K., Segun, G.A. (2016). Effect of hydraulic retention time on anaerobic digestion of Xiao Jiahe municipal sludge. International Journal of Waste Resources, 6(3): 1000231. https://doi.org/10.4172/2252-5211.1000231
[19] Wei, L.L., An, X.Y., Wang, S., Xue, C.H., Jiang, J.Q., Zhao, Q.L., Kabutey, F.T., Wang, K. (2017). Effect of hydraulic retention time on deterioration/restarting of sludge anaerobic digestion: Extracellular polymeric substances and microbial response. Bioresource Technology, 244: 261-269. https://doi.org/10.1016/j.biortech.2017.07.110
[20] Pramanik, S.K., Suja, F.B., Pramanik, B.K. (2020). Effects of hydraulic retention time on the process performance and microbial community structure of an anaerobic single-stage semi-pilot scale reactor for the treatment of food waste. International Biodeterioration & Biodegradation, 152: 104999. https://doi.org/10.1016/j.ibiod.2020.104999
[21] Zhang, X.X., Jiao, P.B., Zhang, M., Wu, P., Zhang, Y.F., Wang, Y.W., Xu, K.Y., Yu, J.Z., Ma, L.P. (2023). Impacts of organic loading rate and hydraulic retention time on organics degradation, interspecies interactions and functional traits in thermophilic anaerobic co-digestion of food waste and sewage sludge. Bioresource Technology, 370: 128578. https://doi.org/10.1016/j.biortech.2023.18578
[22] Okonkwo, U.C., Onokpite, E., Onokwai, A.O. (2018). Comparative study of the optimal ratio of biogas production from various organic wastes and weeds for digester/restarted digester. Journal of King Saud University-Engineering Sciences, 30(2): 123-129. https://doi.org/10.1016/j.jksues.2016.02.002
[23] Li, Y., Ma, J., Yuan, H., Li, X. (2022). Effects of feeding regimes on process performance and microbial community structure in anaerobic semi-continuously stirred tank reactors treating corn stover. Waste and Biomass Valorization, 13: 1003-1014. https://doi.org/10.1007/s12649-021-01573-0
[24] Mohan, S.M., Swathi, T. (2024). Evaluation of the effect of copper on the restart of a novel combined two-stage anaerobic digester. Water and Environment Journal, 38(1): 32-44. https://doi.org/10.1111/wej.12891
[25] Peris Serrano, R. (2010). Biogas process simulation using Aspen Plus. Master Thesis, Syddansk Universitet.
[26] Hoffmann, J., Rudra, S., Toor, S.S., Holm-Nielsen, J.B., Rosendahl, L.A. (2013). Conceptual design of an integrated hydrothermal liquefaction and biogas plant for sustainable bioenergy production. Bioresource Technology, 129: 402-410. https://doi.org/10.1016/j.biortech.2012.11.051
[27] Schefflan, R. (2016). Teach Yourself the Basics of Aspen Plus. John Wiley & Sons.
[28] DaCosta, H., Maohong, F. (2011). Rate Constant Calculation for Thermal Reactions. Wiley, New York.
[29] De Vrieze, J., Verstraete, W., Boon, N. (2013). Repeated pulse feeding induces functional stability in anaerobic digestion. Microbial Biotechnology, 6(4): 414-424. https://doi.org/10.1111/1751-7915.12025
[30] Holman, J.P. (2010). Heat Transfer. McGraw-Hill Education.
[31] Ramasamy, G., Goodman, A.H., Lahuri, H.M., Shah, S.M., Sabil, K.M. (2022). Process simulation of anaerobic digestion for methane production using Aspen Plus. IOP Conference Series: Materials Science and Engineering, 1257(1): 012002. https://doi.org/10.1088/1757-899X/1257/1/012002
[32] Ezemagu, I.G., Ejimofor, M.I., Menkiti, M.C. (2020). Thermodynamic studies of anaerobic digestion of post coagulation sludge from petroleum produced water and cow dung. Current Research in Green and Sustainable Chemistry, 3: 100037. https://doi.org/10.1016/j.crgsc.2020.100037
[33] Saidur, R., Masjuki, H.H., Jamaluddin, M.Y. (2007). An application of energy and exergy analysis in residential sector of Malaysia. Energy Policy, 35(2): 1050-1063. https://doi.org/10.1016/j.enpol.2006.02.006

NOMENCLATURE

Abbreviation

AD	Anerobic digester
AAD	Absolute average deviation
ADM1	Anaerobic digestion model No. 1
CD	Cow dung
PT	Potatoes
d1, d2, d3, d4	Digester numbers 1, 2, 3, and 4, respectively

Symbols

k_f	Kinetic factor (forward reaction) s^{-1}
k_{ff}	Frequency factor direction constant rate s^{-1}
T	Temperature of reaction K
T_o	Reference temperature K
n	Exponent of temperature
E	Active reaction energy kJ/kmole
R	Gas constant kJ/kmole
$\bar{R}$	Universal gas constant kJ/kmole
S_j	Species liquid concentration kmole/m^3

Subscript

i	Input or initial
e	Exit
o	Reference
f	Factor or fuel or formation
ff	Frequency factor
j	Species